



# Asynchronous responses of mechanical and magnetic properties to structure relaxation for FeNbB bulk metallic glass

Zhi-kai Gao<sup>1,2</sup> · An-ding Wang<sup>2,3,4</sup> · Ping-bo Chen<sup>2</sup> · Cheng-liang Zhao<sup>2,3</sup> · Fu-shan Li<sup>1</sup> · Ai-na He<sup>2,3</sup> · Chun-tao Chang<sup>2,3</sup> · Xin-min Wang<sup>2,3</sup> · Chain-tuan Liu<sup>4</sup>

Received: 5 December 2017 / Revised: 9 May 2018 / Accepted: 11 May 2018  
© China Iron and Steel Research Institute Group 2018

## Abstract

Asynchronous responses of mechanical and magnetic properties to structure relaxation for the Fe<sub>71</sub>Nb<sub>6</sub>B<sub>23</sub> bulk metallic glass were systematically investigated. It is interesting that this ternary alloy can combinedly exhibit outstanding magnetic and mechanical properties, especially good ductility, after optimally annealing in structure relaxation stage for eliminating the internal stress and homogenizing the microstructure. The alloy exhibits low coercive force of 1.6 A/m, high effective permeability of  $15 \times 10^3$ , high fracture strength of 4.2 GPa and good plastic strain of 1.8%. It is also found that responses of mechanical and magnetic properties to structure relaxation are asynchronous. The glass transition and crystallization will greatly deteriorate the magnetic and mechanical properties. Here we propose a physical picture and demonstrate that the primary structure factors determining magnetic and mechanical properties are different. This work will bring a promising material for application and a new perspective to study the effect of annealing-induced structure relaxation on mechanical and magnetic properties.

**Keywords** Bulk metallic glass · Annealing · Mechanical property · Magnetic property · Structure relaxation

✉ An-ding Wang  
anding@nimte.ac.cn

✉ Fu-shan Li  
fsli@zzu.edu.cn

✉ Ai-na He  
hean@nimte.ac.cn

<sup>1</sup> School of Materials Science and Engineering, Zhengzhou University, Zhengzhou 450001, Henan, China

<sup>2</sup> Key Laboratory of Magnetic Materials and Devices, Ningbo Institute of Materials Technology and Engineering, Chinese Academy of Sciences, Ningbo 315201, Zhejiang, China

<sup>3</sup> Zhejiang Province Key Laboratory of Magnetic Materials and Application Technology, Ningbo Institute of Materials Technology and Engineering, Chinese Academy of Sciences, Ningbo 315201, Zhejiang, China

<sup>4</sup> Center for Advanced Structural Materials, Department of Mechanical and Biomedical Engineering, College of Science and Engineering, City University of Hong Kong, Hong Kong, China

## 1 Introduction

Bulk metallic glasses (BMGs) have attracted great technological and scientific interests, as a new class of engineering and functional materials, which are increasingly used in various fields like the precise machine parts and electric systems [1, 2]. As produced by rapid quenching of molten metals to prevent crystallization, BMGs are characterized by a non-equilibrium high energy state and structurally by short-range order and long-range disorder. The avoidance of dislocations in this special structure leads to excellent mechanical [3–5], magnetic and chemical properties [6]. For Fe-based BMGs, their outstanding strength and magnetic properties, together with low materials cost, have exposed irresistible application prospect.

As well accepted, the microstructure, energy and stress states of BMGs are not homogeneous [7]. Inhomogeneous structure units like free volume, loose-/dense-packed regions and clusters form in the glassy matrix during the rapid solidification process. These inhomogeneities have proved to be closely related to the properties, especially for the mechanical behaviors and magnetic properties. It is

hence feasible to modulate the properties according to the requirement and explore the microstructure–property connection mechanism. For Fe-based BMGs, annealing is an essential process for eliminating the internal stress and modulating structure. As examined by numerous investigators, the annealing process including the residual stress release and the structural relaxation, together with its effects on magnetic and mechanical properties, is complicated [8, 9]. On one hand, annealing-induced structural relaxation will reduce the number of the free volume and dense-packed regions. The increased structural and chemical homogeneity will greatly decrease the pinning centers of magnetic domains, which directly improve the magnetic properties. On the other hand, the relaxation-induced homogeneity will also lead to the absence of center for inhibiting the shear band slippage and dispersive stress, which determines the ductility [10–12]. It is hence difficult to balance the magnetic and mechanic properties [11]. In some special occasions, both good mechanical and magnetic properties are essential for applications like magnetic head, magnetic cores in the electromagnetic valves, etc. Therefore, the preparation of ductile bulk metallic glass with excellent magnetic and mechanical properties after annealing is quite desired. Though great investigations on the relation between mechanical properties and structural relaxation of BMGs have been carried out and models from different aspects are built, it is still an open question [13–15]. The correlation between microstructure and properties needs to be investigated systematically.

Although a series of Fe-based BMGs with outstanding mechanical or magnetic properties have been documented, only a minority of as-quenched samples exhibit large plasticity. After failing in FeSiBPC [14], FeSiBP [15] and FeMoPCBSi alloys [16], we succeeded in the typical ternary FeNbB alloys which exhibit superb strength [17] and obvious plasticity after annealing. In the study, a ductile Fe<sub>71</sub>Nb<sub>6</sub>B<sub>23</sub> BMG with excellent magnetic and mechanical properties after optimal annealing is reported, which is a proper model material to study the influence mechanism of relaxation on mechanical and magnetic properties. By correlating the macroscopic magnetic and mechanical properties with microstructure, the intrinsic relationship between them was discussed systematically.

## 2 Experimental procedure

Ternary alloy with nominal compositions of Fe<sub>71</sub>Nb<sub>6</sub>B<sub>23</sub> was prepared in an arc furnace with the mixtures of pure Fe (99.99 mass%), Nb (99.99 mass%) and B (99.5 mass%) in an argon atmosphere. The alloy ingots were melted six times to ensure the compositional homogeneity. Glassy alloy ribbons with width of about 1 mm and thickness of

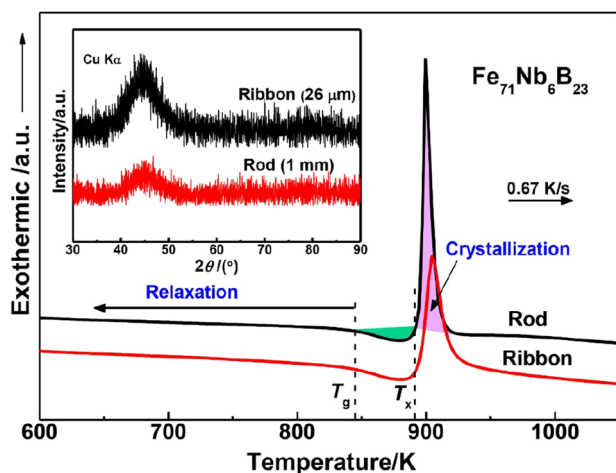
about 26 mm and glassy rods with a diameter of about 1 mm were prepared by single copper roller melt-spinning process and copper mold injection-casting method, respectively. The glassy structures were clearly identified by X-ray diffractometer (XRD, Bruker D8 Advance) with Cu K $\alpha$  radiation. Crystallization behaviors and thermal physical parameters containing glass transition temperature ( $T_g$ ) and crystallization temperature ( $T_x$ ) of the glassy alloy were analyzed by differential scanning calorimeter (DSC, NETZSCH 404C) at a heating rate of 0.67 K/s. As the magnetic properties depend on the sample sizes, ribbon samples with similar size mentioned above were used for measurement to decrease the error. The intrinsic magnetic properties including saturation flux density ( $B_s$ ), coercivity ( $H_c$ ) and effective permeability ( $\mu_e$ ) were measured by vibrating sample magnetometer (VSM, Lake Shore 7410) under an applied field of 800 kA/m, DC  $B$ - $H$  loop tracer (EXPH-100) and impedance analyzer (Agilent 4294 A) under a field of 1 A/m, respectively. The structure of magnetic domains was characterized via the magneto-optical Kerr microscope. Compression tests were carried out for cylindrical rods (1 mm in diameter and 2 mm in length) using a universal testing machine (CMT5205 SANS, China) at a strain rate of  $5 \times 10^{-4} \text{ s}^{-1}$ . At least five samples have been measured to ensure that the results are reproducible. A scanning electron microscope (SEM, FEI quanta FEG 250) was used to characterize the fracture surfaces of the specimens after compression. Vickers hardness tests with ten times for each sample were performed under a load of 4.9 N using a Vickers microhardness tester. Ribbon samples were annealed for 10 min by using an isothermal furnace under a low pressure of about  $5 \times 10^{-3} \text{ Pa}$ . All the magnetic and mechanical property measurements were taken at room temperature. Density of the rod samples with different annealing states was measured by an Archimedes method, using a high precision balance. Three samples with the same state were measured for three times to average out the exact values.

## 3 Results and discussion

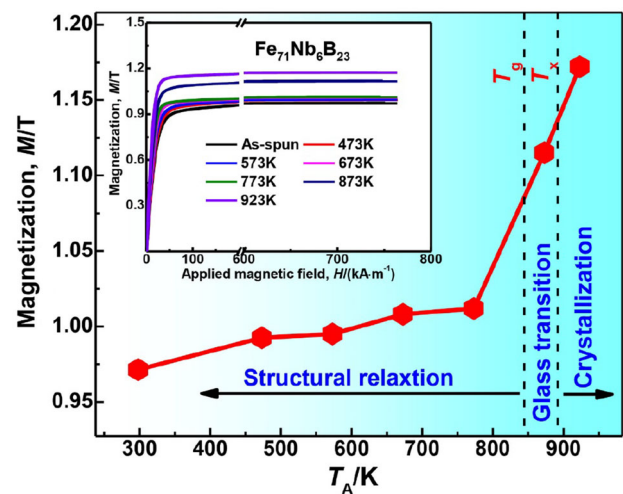
Fe<sub>71</sub>Nb<sub>6</sub>B<sub>23</sub> ribbon samples that were more commonly used in magnetic parts and more convenient for magnetic properties investigation were prepared, since the documented results of the magnetic properties of cast ring samples and spun ribbon samples were similar after annealing [16]. For the investigation of mechanical performance, bulk samples with diameter of 1 mm were cast [17]. The glassy structures were identified by XRD for all ribbon samples with good surface quality and toughness and all rods with uniform size of 1 mm made into powders. As shown in the inset of Fig. 1, the XRD patterns exhibit

only diffuse halos without sharp diffraction peaks corresponding to the crystalline phases. This result confirms that the alloy has good glass-forming ability (GFA) and is suitable to be used as a model material for studying structural relaxation. As shown in Fig. 1, DSC curves of the  $\text{Fe}_{71}\text{Nb}_6\text{B}_{23}$  glassy ribbon and rod are almost the same, except the intensity of the single crystallization peak. The similar characteristic temperatures containing  $T_g$ ,  $T_x$  and  $\Delta T_x$  ( $T_x - T_g$ ) illuminate weak effects of the cooling rate on critical structural transition for fully glassy samples. According to the previous report [18], the structural transitions can be divided into three stages: structural relaxation stage, glass transition stage and crystallization stage. The dependence of annealing temperature ( $T_A$ ) on magnetic and mechanical properties was then studied.

The  $B_s$  reflecting the magnetic interaction between Fe atoms was investigated in detail [19]. Inset of Fig. 2 shows the hysteresis loops measured with VSM for the samples annealed for 10 min at different temperatures. The  $B_s$  values are summarized and shown in Fig. 2, and the curve shows rising tendency with the increase in  $T_A$ . It should also be noted that the amplifications in the glass transition and crystallization stages are much larger than those in structural transition stage. The exchange coupling interaction of magnetic atoms is mainly affected by the distance between Fe atoms, the bond state, free volume annihilation, formation and dissolution of clusters and phases in these three stages, which greatly affect the  $B_s$  [19]. During the structural relaxation stage, the free volume decreases considerably and ferromagnetic atoms are closer to each other, resulting in a slight increase in  $B_s$ . When annealed in the glass transition stage, some clusters will dissolve and lead to the breaking of bonds, resulting in the increase in Fe atoms with unfilled  $3d$  electrons, leading to a sharp



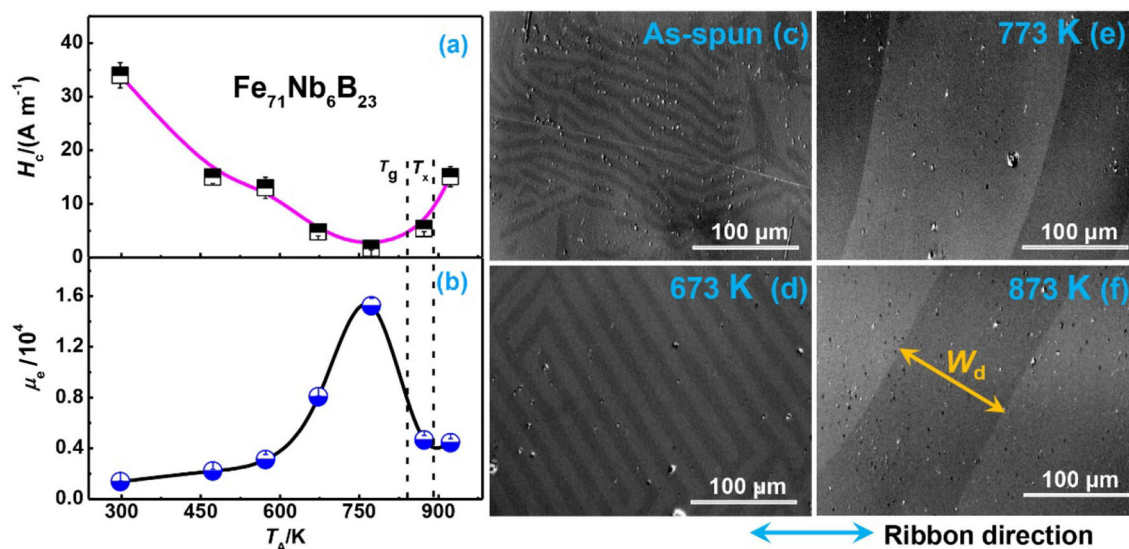
**Fig. 1** DSC curves of  $\text{Fe}_{71}\text{Nb}_6\text{B}_{23}$  glassy alloy ribbon and rod at a heating rate of 0.67 K/s. Inset shows XRD patterns of as-prepared ribbons and rods



**Fig. 2**  $T_A$  dependence of  $B_s$ . Inset shows hysteresis loops measured with VSM

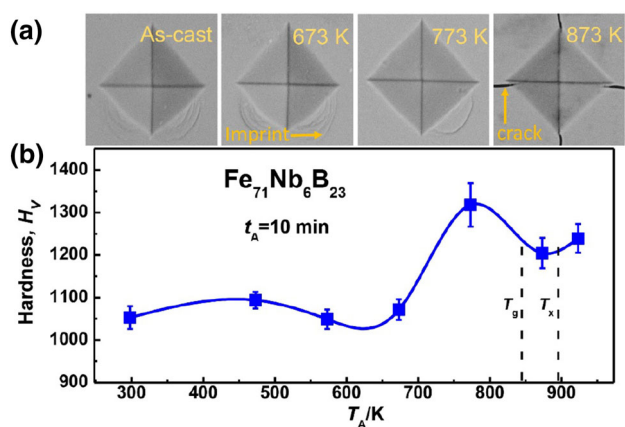
increase in  $B_s$ . In the crystallization stage, the randomly distributed Fe atoms will become ordered in  $\alpha$ -Fe and compounds. The obvious increase in  $B_s$  also indicates the formation of  $\alpha$ -Fe phase or clusters.

Figure 3a,b shows the  $T_A$  dependence of  $H_c$  and  $\mu_c$  for  $\text{Fe}_{71}\text{Nb}_6\text{B}_{23}$  glassy alloy ribbons annealed for 10 min. As seen in Fig. 3a,  $H_c$  of the alloy decreases with the increase in  $T_A$  in the relaxation stage. The  $H_c$  reaches the lowest value of 1.6 A/m after annealed at 773 K, which can be attributed to the stress release and structure relaxation [20]. The trend of  $\mu_c$  of the alloy in the relaxation stage with the increase in  $T_A$  is contrary to that of the  $H_c$ . The  $\mu_c$  also reaches the highest value of  $15 \times 10^3$  at 773 K. The internal stresses, free volume and the loose-/dense-packed regions play an important role in the configuration of the domain structure, which affect the magnetic properties greatly [21]. The structural relaxation induced by annealing leads to the decrease in the free volume and the release of stress, which improve soft magnetic properties [22]. When  $T_A$  is higher than  $T_g$ , the  $H_c$  increases and  $\mu_c$  decreases drastically, illustrating that the glass transition and crystallization will deteriorate the soft magnetic properties of the glassy alloy. In order to thoroughly understand the transition of soft magnetic properties, the magnetic domain structure was then identified. As shown in Fig. 3c–e, the irregular stripe domains change into regular stripe domains in the structure relaxation stage, indicating that the annealing leads to the release of stress and the decrease in free volume. The magnetic domain walls can move and rotate easily, and energy of the domain wall is reduced, which is consistent with the improvement of  $H_c$  and  $\mu_c$  [23]. For the sample which has suffered glass transition, the width of the stripe domain decreases, indicating a higher pinning effect by the clusters.



**Fig. 3**  $T_A$  dependence of  $H_c$  (a) and  $\mu_e$  (b) of  $\text{Fe}_{71}\text{Nb}_6\text{B}_{23}$  glassy alloy ribbons annealed for 10 min, and magnetic domain images of ribbon samples with different states (c–f)

Hardness measurement has been conducted by applying a load of 4.9 N for 10 s. More than ten indentations were carried out to obtain the average  $H_V$  values. As shown in Fig. 4a, a number of slip steps around the indenter imprints can be seen in the samples annealed below 773 K, indicating the good plasticity of these samples [24]. For the samples after glass transition and crystallization, cracks can be easily observed around the indentation, showing the reduced ductility. As shown in Fig. 4b, the  $H_V$  of the alloy is almost unchanged in the low-temperature relaxation process. When the  $T_A$  reaches 773 K, an obvious increase is clearly seen. It is interesting to note that the highest  $H_V$  and the best soft magnetic properties are obtained in the same samples correlated with the optimal  $T_A$  of 773 K. It is hence feasible to dilute that the annihilations of free volume and loose-/dense-packed regions lead to a more



**Fig. 4** Optical microscopy images of indentations imprints of samples with different states (a) and  $T_A$  dependence of hardness of rod samples annealed for 10 min (b)

homogeneous microstructure. Accompanied with the plasticity reduction, the  $H_V$  decreases obviously for the samples annealed at  $T_A$  higher than  $T_g$  and  $T_x$ . Since only a partial crystallization occurred and a composite was formed, the decrease in  $H_V$  and plasticity is understandable.

Figure 5a presents the compressive nominal stress–strain curves of the  $\text{Fe}_{71}\text{Nb}_6\text{B}_{23}$  glassy rods with 1 mm

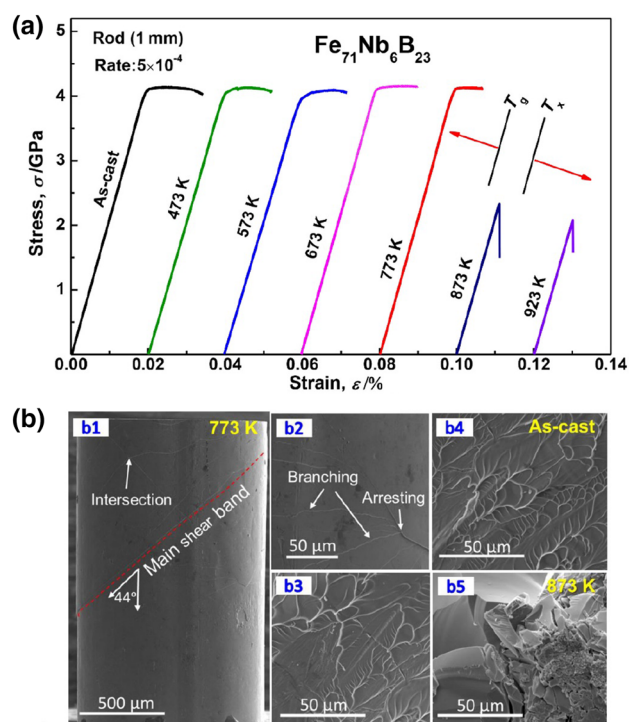


**Fig. 5** Compressive stress–strain curves (a) and SEM images (b) of fracture features of rod samples annealed for 10 min

diameter annealed for 10 min. It can be seen that the samples exhibit high strength of about 4.2 GPa and good ductility even after annealing in the structure relaxation stage. Ductile FeNbB bulk metallic glass with excellent magnetic and mechanical properties was successfully prepared after annealing optimization. It is generally believed that annealing will lead to the decrease in free volume and loose-packed regions, which will greatly decrease the ductility of the glassy alloys. This result is quite different from that of the general Fe-based BMGs with brittle nature even in as-cast state, however, illustrating that it is feasible to combinedly obtain BMGs with excellent soft magnetic and mechanical properties. After glass transition and crystallization, the samples fracture without reaching the yield point indicates that the original stable structure is destroyed. It is hence supposed that the free volume decreases greatly in the relaxation stage, while the dense-packed and ordered structure still maintain a high number, which act as the origins for ultrahigh resistance against fracture and plastic yielding.

The fracture features for Fe<sub>71</sub>Nb<sub>6</sub>B<sub>23</sub> metallic glass after failure are revealed in Fig. 5b. The outer and fracture surface of the samples after relaxation shows some shear bands and well-defined vein patterns (as seen in Fig. 5b1–b4), respectively. These patterns often reflect the local viscous flow of glassy metals and only occur in those BMGs with good ductility [25]. Localized main shear band appears and ends up at the sample side in Fig. 5b1, which is characterized by a shear angle of about 44° to the compressive axis. It is noted that several scattered shear bands are presented in Fig. 5b2. The formation of many shear bands gives a hint that the Fe<sub>71</sub>Nb<sub>6</sub>B<sub>23</sub> BMG holds a definite resistance to catastrophic failure after structural relaxation. Thus, the Fe<sub>71</sub>Nb<sub>6</sub>B<sub>23</sub> glassy alloy evidently verifies its good ductility corresponding to the stress–strain curve. Owing to the crystallization of the alloy after annealed at 873 K, the fracture surface of the alloy is very smooth (as seen in Fig. 5b5), and the fracture morphology is a typical brittle fracture. The fracture surface morphologies of the alloy annealed at different temperatures are consistent with the results of stress–strain curves.

The above-mentioned results provide convincing evidence that the magnetic and mechanical properties were mechanistically related to different primary structure factors, especially in the structure relaxation stage. To verify this viewpoint, attention was paid to the analysis of Bitoh et al. [26], in which the free volume is correlated with the main sources of elastic stress and quasidislocation dipole-type defects. The origin of the optimal soft magnetic properties corresponds to the reduced density and size of free volume and poor pinning effect of domain walls. A density measurement was taken, which proved to be a reliable and easy way to characterize the structure

relaxation, glass transition and crystallization stages [27]. Figure 6a displays the  $T_A$  dependence of density ( $\rho$ ) for the annealed glassy and crystallized samples. It is clear that the structure relaxation at low  $T_A$  does not lead to obvious  $\rho$  increase, implying that no distinct structure change happens. For the sample exhibiting optimal soft magnetic properties, the  $\rho$  increases slightly, manifesting the free volume annihilation. The thorough free volume elimination should be the reason of poor pinning effect of domain walls and optimal softness. The much more obvious  $\rho$  increases in the samples after glass transition and crystallization show the large structure changes. The underpinning physics behind present experimental observations was discussed then. As illustrated in Fig. 6b, the following pictures were proposed to explain the correlations between structure transition and properties. As suggested in many papers, the annealing reduced structure relaxation can homogenize composition, release internal stress and reduce free volume [28], which is beneficial to soft magnetic properties, but deteriorates ductility of the alloy. The improved soft magnetic properties after structural relaxation are shown in Fig. 3a,b. Due to the reduction of free volume in the relaxation stage, the structure of glassy alloy becomes more compact [28], and the  $B_s$  and hardness are slightly increased corresponding to the changes of those in Figs. 2 and 4b, respectively. The free volume and the dense-packed structure are dominant for the mechanical properties, compared with the internal stress. As shown in Fig. 6b, during the relaxation stage, a large number of dense-packed structures still remain in the alloy, which is the reason for the remaining plasticity of the alloy. These remaining dense-packed structures can impede the movement of shear bands and play a role in dispersing and proliferating shear bands (see Fig. 5b2), resulting in the improved plasticity and toughness of the alloy. During the glass transition and crystallization stages, a large number of dense-packed structures annihilate, and then, the atoms rearrange and crystallize, leading to a sharp decrease in the strength and ductility [29]. In the end, the  $\alpha$ -Fe and borides have been generated, leading to a pronounced increase in  $B_s$ , which is consistent with the glass transition and crystallization stages of  $B_s$  in Fig. 2. As indicated in the mechanism diagram, the effects of annealing on mechanical and magnetic properties at different stages are different. The temperature asynchronism between mechanical and magnetic properties of glassy alloy is promising to obtain excellent performance by controlling the heat treatment process.

Finally, the reason why Fe<sub>71</sub>Nb<sub>6</sub>B<sub>23</sub> BMG can achieve optimal soft magnetic properties without suffering thermal embrittlement, which is commonly reported in Fe-based BMGs, is further addressed. Although the origin of the plasticity for BMGs and its influence mechanism of the

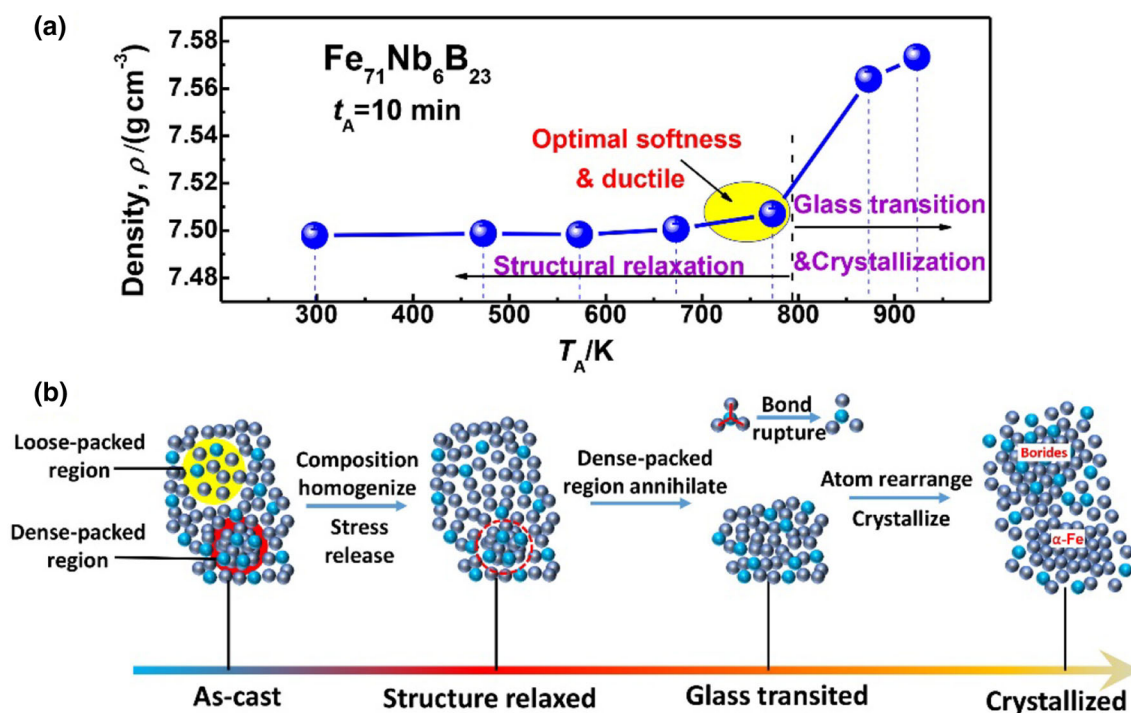


**Fig. 6** Illustrated mechanisms of microstructural transitions of  $\text{Fe}_{71}\text{Nb}_6\text{B}_{23}$  glassy alloy at different annealing stages

compositions are still not clear, the reasons can be explored as follows. First, compared with the typical  $\text{Fe}_{76}\text{Si}_9\text{B}_{10}\text{P}_5$ ,  $\text{Fe}_{76}\text{Mo}_{3.5}\text{P}_{10}\text{C}_4\text{B}_4\text{Si}_{2.5}$  and  $\text{Fe}_{78}\text{Si}_9\text{B}_{13}$  BMGs, the as-cast  $\text{Fe}_{71}\text{Nb}_6\text{B}_{23}$  BMG exhibits larger plasticity which has higher potential to remain after annealing. Second,  $\text{Fe}_{71}\text{Nb}_6\text{B}_{23}$  exhibits high content of Nb with high Poisson ratio and does not contain low Poisson ratio elements like Si and P, which may result in a comparatively high Poisson ratio. Third, it has been reported that the initial precipitation phase of the  $\text{Fe}_{71}\text{Nb}_6\text{B}_{23}$  BMG is  $\text{Fe}_{23}\text{Nb}_6$  which has very complicated structure and large size. The clusters in the as-cast rod samples should also exhibit much more complicated structure and be more stable. During the annealing process, the clusters are stable and will inhibit the large structure transition of the glassy phase, except through free volume annihilation. At last, it should be noted that the annealing-induced brittleness of the BMG is still an open and important issue. The present study just gives an experimental result, and speculations and further investigations are still desired.

## 4 Conclusions

1. This ternary alloy can combinedly exhibit outstanding soft magnetic and mechanical properties after optimally annealing, including low  $H_c$  of 1.6 A/m, high  $\mu_e$

of  $15 \times 10^3$ , high fracture strength of 4.2 GPa and good plastic strain of 1.8%.

2. The influence of the change of structural units on the magnetic and mechanical properties is asynchronous. During structure relaxation stage, the decrease in free volume is beneficial to soft magnetic properties but deteriorates ductility, and a large number of dense-packed structures still remain in the alloy, which is the origin of the plasticity. During the glass transition and crystallization stages, the atoms rearrange and crystallize, leading to a sharp decrease in the strength and ductility.

**Acknowledgements** This work was mainly supported by the National Key Research and Development Program of China (Grant Nos. 2016YFB0300501, 2017YFB0903902), and the National Natural Science Foundation of China (Grant Nos. 51601206, 51771159). Anding Wang and Chain-tsuan Liu would like to acknowledge the support by General Research Fund of Hong Kong under the grant number of City 102013.

## References

- [1] W.H. Wang, C. Dong, C.H. Shek, *Mater. Sci. Eng. R* 44 (2004) 45–89.
- [2] W.F. Wu, Y. Li, C.A. Schuh, *Philos. Mag.* 88 (2008) 71–89.
- [3] A. Inoue, B.L. Shen, H. Koshida, H. Kato, A.R. Yavari, *Nat. Mater.* 2 (2003) 661–663.
- [4] C.J. Gilbert, R.O. Ritchie, W.L. Johnson, *Appl. Phys. Lett.* 71 (1997) 476–478.

- [5] A.R. Yavari, J.J. Lewandowski, J. Eckert, *MRS Bull.* 32 (2007) 635–638.
- [6] D. Zander, B. Heisterkamp, I. Gallino, *J. Alloy. Compd.* 434 (2007) 234–236.
- [7] W. Li, Y. Gao, H. Bei, *Sci. Rep.* 5 (2015) 14786.
- [8] A. Castellero, B. Moser, D.I. Uhlenhaut, F.H. Dalla Torre, J.F. Loeffler, *Acta Mater.* 56 (2008) 3777–3785.
- [9] L. Hu, Y. Yue, *J. Phys. Chem. C* 113 (2009) 15001–15006.
- [10] K.J. Laws, D. Granata, J.F. Loeffler, *Acta Mater.* 103 (2016) 735–745.
- [11] Y.C. Niu, X.F. Bian, W.M. Wang, *J. Non-Cryst. Solids* 341 (2004) 40–45.
- [12] X.H. Xu, G. Wang, F.J. Ke, W.H. Wang, *Scripta Mater.* 59 (2008) 657–660.
- [13] C.A. Schuh, T.C. Hufnagel, U. Ramamurty, *Acta Mater.* 55 (2007) 4067–4109.
- [14] A. Makino, C. Chang, T. Kubota, A. Inoue, *J. Alloy. Compd.* 483 (2009) 616–619.
- [15] J. Zhang, C. Chang, A. Wang, B. Shen, *J. Non-Cryst. Solids* 358 (2012) 1443–1446.
- [16] M.X. Zhang, A.D. Wang, B.L. Shen, *AIP Adv.* 2 (2012) 022169.
- [17] J.H. Yao, J.Q. Wang, Y. Li, *Appl. Phys. Lett.* 92 (2008) 251906.
- [18] O. Haruyama, K. Sugiyama, M. Sakurai, Y. Waseda, *J. Non-Cryst. Solids* 353 (2007) 3053–3056.
- [19] A. Wang, C. Zhao, A. He, H. Men, C. Chang, X. Wang, *J. Alloy. Compd.* 656 (2016) 729–734.
- [20] X. Liang, A. He, A. Wang, J. Pang, C. Wang, C. Chang, K. Qiu, X. Wang, C.T. Liu, *J. Alloy. Compd.* 694 (2017) 1260–1264.
- [21] O. Životský, A. Hendrych, L. Klimša, Y. Jirásková, J. Buršík, J.A.M. Gómez, D. Janičkovič, *J. Magn. Magn. Mater.* 324 (2012) 569–577.
- [22] Q. Hu, X.R. Zeng, M.W. Fu, *J. Appl. Phys.* 109 (2011) 053520.
- [23] C. Zhao, A. Wang, A. He, S. Yue, C. Chang, X. Wang, R.W. Li, *J. Alloy. Compd.* 659 (2016) 193–197.
- [24] P. Denis, C.M. Meylan, C. Ebner, A.L. Greer, M. Zehetbauer, H.J. Fecht, *Mater. Sci. Eng. A* 684 (2017) 517–523.
- [25] A. Inoue, *Acta Mater.* 48 (2000) 279–306.
- [26] T. Bitoh, A. Makino, A. Inoue, *J. Appl. Phys.* 99 (2006) 08F102.
- [27] V.M. Giordano, B. Ruta, *Nat. Commun.* 7 (2016) 8.
- [28] Q. Wang, S.T. Zhang, Y. Yang, Y.D. Dong, C.T. Liu, J. Lu, *Nat. Commun.* 6 (2015) 7876.
- [29] G.R. Garrett, M.D. Demetriou, M.E. Launey, W.L. Johnson, *Proc. Natl. Acad. Sci. USA* 113 (2016) 10257–10262.